Alzheimer's & Dementia: Diagnosis, Assessment & Disease Monitoring 6 (2017) 21-30

Alzheimer's & Dementia

PART II. State of the Field: Advances in Neuroimaging from the 2016 Alzheimer's Imaging Consortium

Tau-PET uptake: Regional variation in average SUVR and impact of amyloid deposition

Prashanthi Vemuri[a,*], Val J. Lowe[a], David S. Knopman[b], Matthew L. Senjem[a], Bradley J. Kemp[a], Christopher G. Schwarz[a], Scott A. Przybelski[c], Mary M. Machulda[d], Ronald C. Petersen[b], Clifford R. Jack, Jr.[a]

[a]*Department of Radiology, Mayo Clinic, Rochester, MN, USA*
[b]*Department of Neurology, Mayo Clinic, Rochester, MN, USA*
[c]*Department of Health Sciences Research, Mayo Clinic, Rochester, MN, USA*
[d]*Department of Psychology, Mayo Clinic, Rochester, MN, USA*

Abstract

Introduction: Tau-positron emission tomography (PET) imaging with AV1451 is sensitive to Alzheimer disease (AD)–related tau deposition in the brain. We (1) examined regional variation of average tau-PET standardized uptake value ratios (SUVRs) in a young normal population (30–49 years) and corrected for the regional variability and (2) tested if the standardized values (z-scores) scaled appropriately to capture regional Alzheimer-specific (i.e., amyloid sensitive) tau-PET changes in individuals aged 50+ years.

Methods: We identified 490 individuals (70 between 30–49 years as a reference group and 420 cognitively normal between 50–95 years of age) with tau-PET and amyloid PET scans from the Mayo Clinic Study of Aging.

Results: There was intrinsic regional variability in average tau-PET SUVR with uptakes higher in some regions than others, even in the younger individuals who would have minimal or no neurofibrillary tangles. We corrected for this using region of interest–specific z-scores based on the reference group. Amyloid and tau-PET uptake were associated throughout the brain after adjusting for age, with the highest correlations in the medial temporal regions.

Discussion: Regions with high-average SUVR are not necessarily those with the greatest tau pathology. Standardization is therefore recommended. Standardization of the data "realigns" the data such that the regional tau z-scores are informative of the disease process, that is, regions with high z-scores now coincide with regions correlated with amyloid deposition. Medial temporal structures, specifically entorhinal cortex–tau, may be useful as an AD-specific tau-PET signature due to its sensitivity to amyloid.

Keywords: Alzheimer disease; Tau imaging; Amyloid imaging

1. Introduction

The pathological hallmarks of Alzheimer disease (AD) are neuritic plaques composed of β-amyloid fibrils and neurofibrillary tangles composed of hyperphosphorylated tau. In vivo imaging of these pathologies has been very useful in understanding the pathological basis of cognitive dysfunction. Pittsburgh compound B (PiB) positron emission tomography (PET) imaging, the first ligand for imaging amyloid, provides an in vivo measure of Aβ burden [1]. PiB-PET binds to insoluble (fibrillary) amyloid beta deposits and has been validated in autopsy studies [2,3]. In contrast,

*Corresponding author. Tel.: +1 507 538 0761; Fax: +1 507 284 9778.
E-mail address: vemuri.prashanthi@mayo.edu

http://dx.doi.org/10.1016/j.dadm.2016.12.010

tau-PET ligands have recently been developed, with AV1451 being the most studied at this point [4–11]. Autoradiography studies have confirmed that tau-PET imaging via 18F-AV-1451 (or AV1451) binds most strongly to 3R/4R paired-helical filament tau deposits seen specifically in AD and only weakly or not at all to straight tau filaments seen in primary non-AD tauopathies. AV1451 does not bind at all at concentrations used in imaging to other common protein aggregates such as beta amyloid and synuclein [12–14].

PET imaging has significantly evolved over the last 4 decades. However, the intrinsic stochastic nature of the PET acquisition process as discussed in the following adds variability to the quantified PET images widely used. There are four main components of PET imaging: (1) PET radiotracer that is injected and accumulates in the target of interest. For example, 11C-PiB binds to fibrillar β–amyloid deposits, and AV1451 has high binding affinity for fibrillar tau deposits present in AD; (2) PET scintillation crystals that detect incident photons that emerge from positron tracer decay; (3) image reconstruction that reconstructs the spatial distribution of radiotracer decay from the incident photons on the detectors, making assumptions about the data acquisition process; (4) image quantitation that includes attenuation correction and quantification using image processing methods. Intrinsically, the variability in the PET data arises from the uncertainty in the detected data due to positron decay, attenuation, scatter, and random events, and the PET detection process [15]. Although several corrections are made to the acquired data, the signal-to-noise ratio and spatial resolution (∼6 mm) [16] are reflective of the uncertainty and noise in the PET data. In addition, there can be biological variability in the PET data due to dependence on blood flow for delivery of the tracer to the brain and partial volume effects due to neurodegeneration [17]. Standardized uptake value ratio (SUVR) is the most common quantitative method used to make regional comparisons within a subject as well as between subjects and computed as the degree of radiotracer uptake in a target region of interest with respect to a reference region. In amyloid and tau imaging, SUVR is typically generated using some portion or the entire cerebellum as a reference because cerebellum is not affected until late in the progression of AD.

We hypothesized that there is significant intrinsic regional variation in the mean tau-PET SUVR (for a variety of reasons—both biological and technical) even in subjects with little tau deposition which in turn will have a significant impact on the interpretation of tau images where significant tracer uptake is present. Also, this variability in average SUVR will have an impact on understanding amyloid effects on tau uptake. Therefore, the goal of this study was two-fold: (1) to examine the regional variation of average tau-PET SUVR (measure via AV1451) in a young normal population (30–49 years) and identify a method to correct for this and (2) to test if the standardized values (z-scores) scale appropriately to capture regional Alzheimer-specific (i.e., amyloid sensitive) tau-PET changes in a population-based cohort (50+ years individuals). We used cognitively normal participants from the Mayo Clinic Study of Aging (MCSA) aged 30 years and older to answer these two questions.

2. Methods

2.1. Selection of participants

All study participants were from the Mayo Clinic Study of Aging, an epidemiological study of the prevalence, incidence, and risk factors for mild cognitive impairment among Olmsted County, MN residents aged 50–89 years. Recently, individuals between 30 and 49 years were also enrolled. The sampling frame for the MCSA is based on the Rochester Epidemiology Project medical records–linkage system [18,19], and residents are randomly selected from the county for participation based on age and sex strata. We included all 70 individuals aged 30–49 years who had tau-PET scans as the reference group and all 420 individuals (50–94 years) who had tau-PET and PiB-PET available and were cognitively normal. More extensive details of the MCSA design and diagnosis have been published elsewhere [20,21].

2.1.1. Standard protocol approvals, registrations, and patient consents

These studies were approved by the Mayo Clinic and Olmsted Medical Center institutional review board. Informed consent was obtained from all participants or their surrogates.

2.2. AD imaging biomarker outcomes

2.2.1. Amyloid and tau pathology assessment from PET scans

PiB-PET and tau-PET images were acquired with a PET/CT operating in three-dimensional mode. The details of the acquisition and processing were published previously [22]. Broadly speaking, an in-house modified version of the automated anatomic labeling atlas was used and the atlas-based parcellation of the PET images into regions of interest was done in the subject's native anatomical space.

2.2.1.1. Amyloid deposition

Global cortical PIB-PET retention ratio was computed as previously reported: the median uptake of voxels in the prefrontal, orbitofrontal, parietal, temporal, anterior cingulate, and posterior cingulate/precuneus regions of interest (ROIs) for each subject were divided by the median uptake over voxels in the cerebellar gray-matter ROI of the atlas [23]. We used a global SUVR cutoff of 1.4 to determine amyloid abnormality or positivity [24].

2.2.1.2. Tau deposition

Regional uptake of tau-PET was assessed in 46 atlas regions by summarizing the median uptake in each region scaled to the median uptake in the cerebellar crus (SUVR)

[25]. For the main analysis, we did not partial volume correct the tau-PET signal and but did conduct a parallel sensitivity analyses using partial volume–corrected data.

2.3. Statistical methods

We described characteristics of the reference group participants (30–49) and 50+ using standard summary measures (means and standard deviations [SDs] for continuous variables, and counts and percentages for categorical variables).

2.4. Regional variability of tau-PET SUVR

We plotted the regional average SUVR in the 30- to 49-year-old reference group by decade as well as in the 50+ individuals. We also computed the coefficient of variation (CV) of the raw SUVRs in the reference group by dividing the SD by the mean SUVR in each region. Then, we converted the raw SUVRs into z-scores using tau-PET scans of the reference group. This allowed us to standardize the SUVR values by accounting for the intrinsic average regional variation. In a sensitivity analysis, we also evaluated the effect of the average size of the ROI on the CV and mean SUVR in each region.

2.5. Amyloid associations with regional tau-PET uptake

We estimated partial correlations between global amyloid and regional tau-PET SUVR after accounting for age. In addition to using the z-score data, we also classified brain regions as positive and negative using a cutoff of 2. A cutoff of 2 corresponds to the 97.5th percentile in the reference group and, when applied to individuals in the 50+ group, a test with 97.5% specificity.

3. Results

The participant characteristics of the reference group (30–49) and 50+ individuals are shown in Table 1.

3.1. Regional variation of tau-PET SUVR

The mean and 95% confidence interval of the average tau-PET SUVR and the CV (which is SD over mean) in 46 atlas regions of the reference group is shown in Fig. 1. SUVR values are displayed separately by decade (30–39 by blue circles; 40–49 by green diamonds) in the reference group. The plot of SUVR by decade illustrates the minimal tau deposition observed in 30- to 49-year-old individuals. Roughly speaking, across regions, these subjects tended to have uptake levels about 10% higher than in the cerebellum corresponding to SUVR levels around 1.1. Despite the overall low-average SUVRs, occipital and frontal regions tended to have higher mean SUVR compared to medial temporal regions.

Table 1
Characteristics of participants in the reference group (30–49) and in main analyses (50–90+)

Characteristics	30–49 (n = 70)	50–90+ (n = 420)
Demographics		
Age, years, mean (SD) [min, max]	40 (6) [30, 49]	72 (10) [52, 94]
Male gender, no. (%)	36 (51)	228 (54)
Education, years, mean (SD) [min, max]	16 (2) [12, 20]	15 (2) [7, 20]
APOE ε4 positive, no. (%)	5 (19)*	114 (27)
Biomarker outcomes		
PiB, SUVR, mean (SD) [min, max]	1.20 (0.05) [1.10, 1.35]	1.47 (0.33) [1.12, 3.08]
Abnormal PiB (>1.4), no. (%)	0 (0)	154 (37)
Cognition		
Short test of mental status score, mean (SD) [min, max]	37 (2) [32, 38]	36 (2) [27, 38]

Abbreviations: SD, standard deviation; PiB, Pittsburgh compound B; SUVR, standardized uptake value ratio.
*Several missing *APOE* genotype.

We found no evidence that 40- to 49-year-olds had higher levels than 30- to 39-year-olds in the cortex except sampling variability and therefore pooled this group to obtain more stable mean and SD estimates for Z-score transformations. The CV plot is shown in the right panel of Fig. 1. The range of CV in different regions reflects more versus less heterogeneity across subjects relative to the sample mean. With the exception of the central gray regions and amygdala, the CV was below 0.1 or 10% in all the other brain regions.

In Fig. 2, the average regional tau-PET SUVRs in the 50+ individuals are shown in the first panel, and the computed average regional tau-PET z-scores (z-scored) are shown in the second panel. Given that a z-score of 0 represents a tau level corresponding to the average tau in 30- to 49-year-old individuals, the average z-scores in 50+ individuals were greater than zero in most brain regions except the postcentral and the Heschl gyri. The increased z-scores in the 50+ group are in line with the expected tau accumulation occurring with age, that is, greater average tau z-scores (greater than 1) in the temporal regions compared to the frontal, occipital, and parietal lobes and lower tau z-scores in the sensorimotor regions.

Average tau-PET SUVRs and z-scores in the entorhinal cortex (ERC), inferior temporal lobe, and pallidum are shown in Fig. 3. Before standardization of the SUVRs (the top panel in Fig. 3), the inferior temporal SUVR appears to increase more as individuals age with higher mean SUVR and a nearly linear increase with age compared to ERC. However, the standardization (bottom

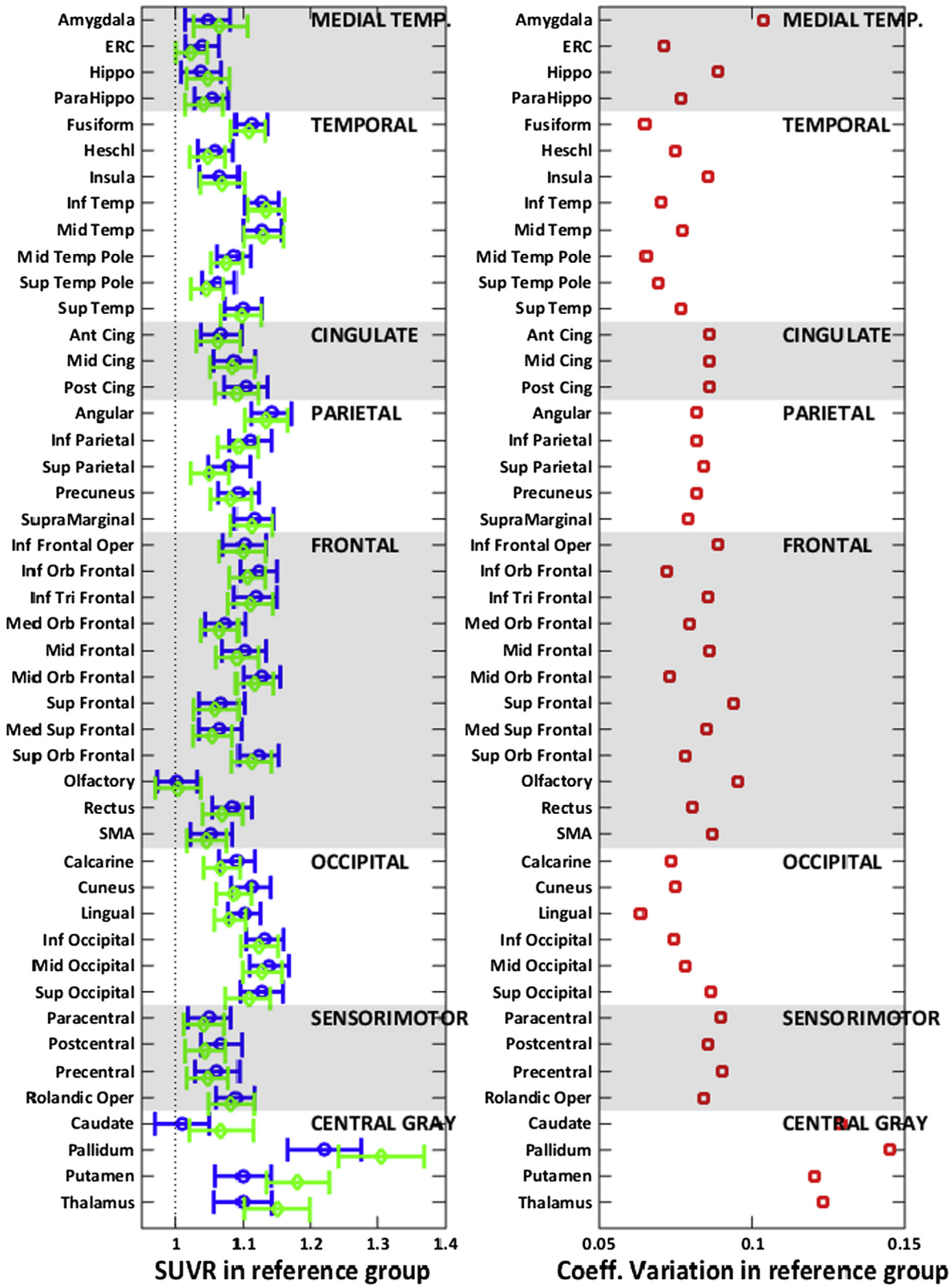

Fig. 1. (Left panel) Average tau-PET SUVR in 46 atlas regions in the reference group (30–49 years). The blue circles show the SUVR in 30–39 group and the green diamonds show the SUVR in the 40–49 group. The means and 95% confidence intervals are shown as error bars for each region. (Right panel) Coefficient of variation defined as the SD of the SUVR values divided by the mean of the SUVR values in 46 atlas regions in the reference group (30–49 years). All regions are ordered and grouped as subgroups of larger areas shown on each of the plots. Abbreviations: ERC, entorhinal cortex; SMA, supplementary motor area; SD, standard deviation; SUVR, standardized uptake value ratio.

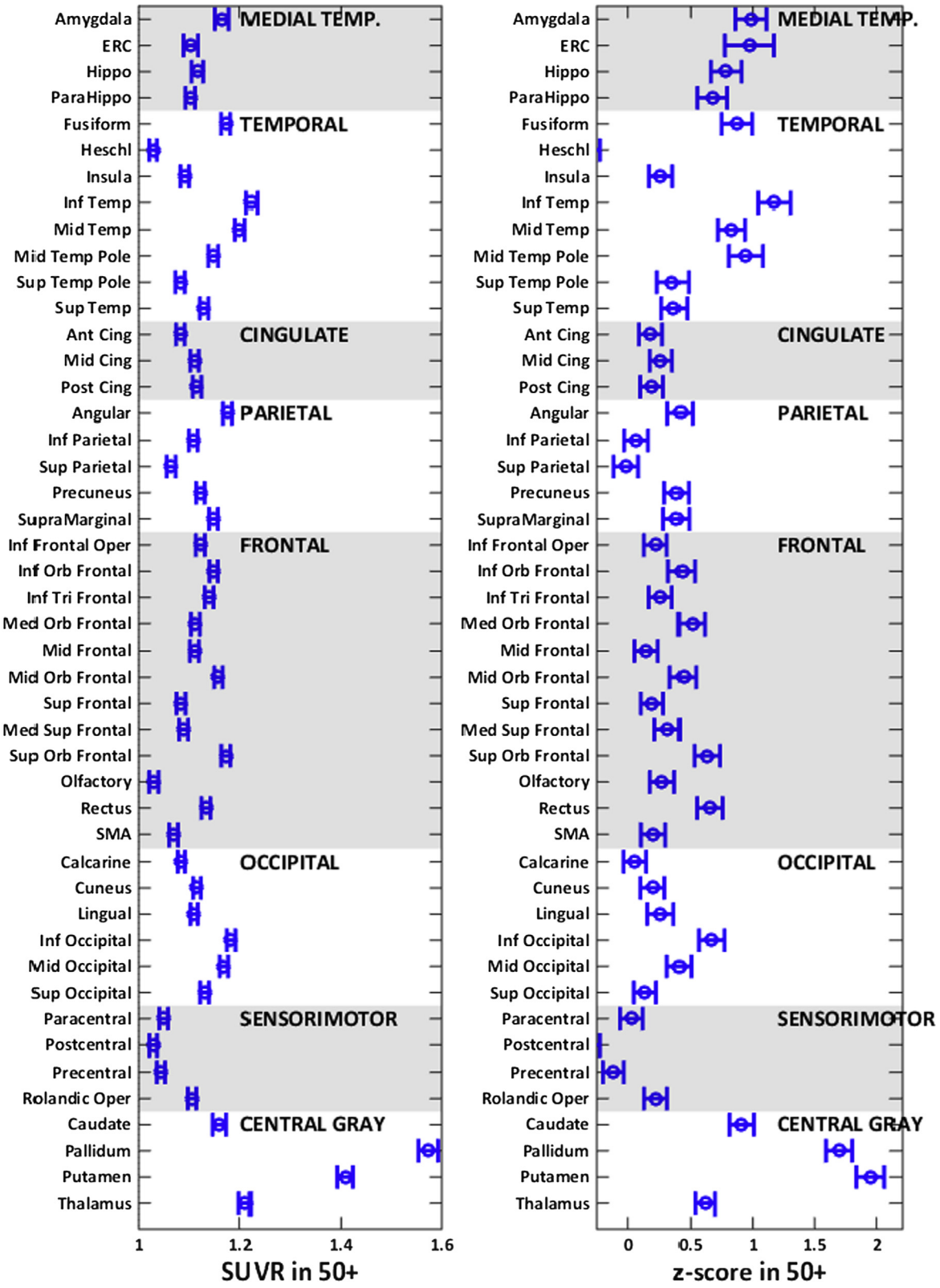

Fig. 2. Average tau-PET SUVR (left panel) and z-scores (right panel) in 46 atlas regions in the 50+ individuals. The means and 95% confidence intervals are shown as error bars for each region. These regions are ordered and grouped as subgroups of larger anatomic areas shown on each of the plots. Abbreviations: ERC, entorhinal cortex; SMA, supplementary motor area; SUVR, standardized uptake value ratio.

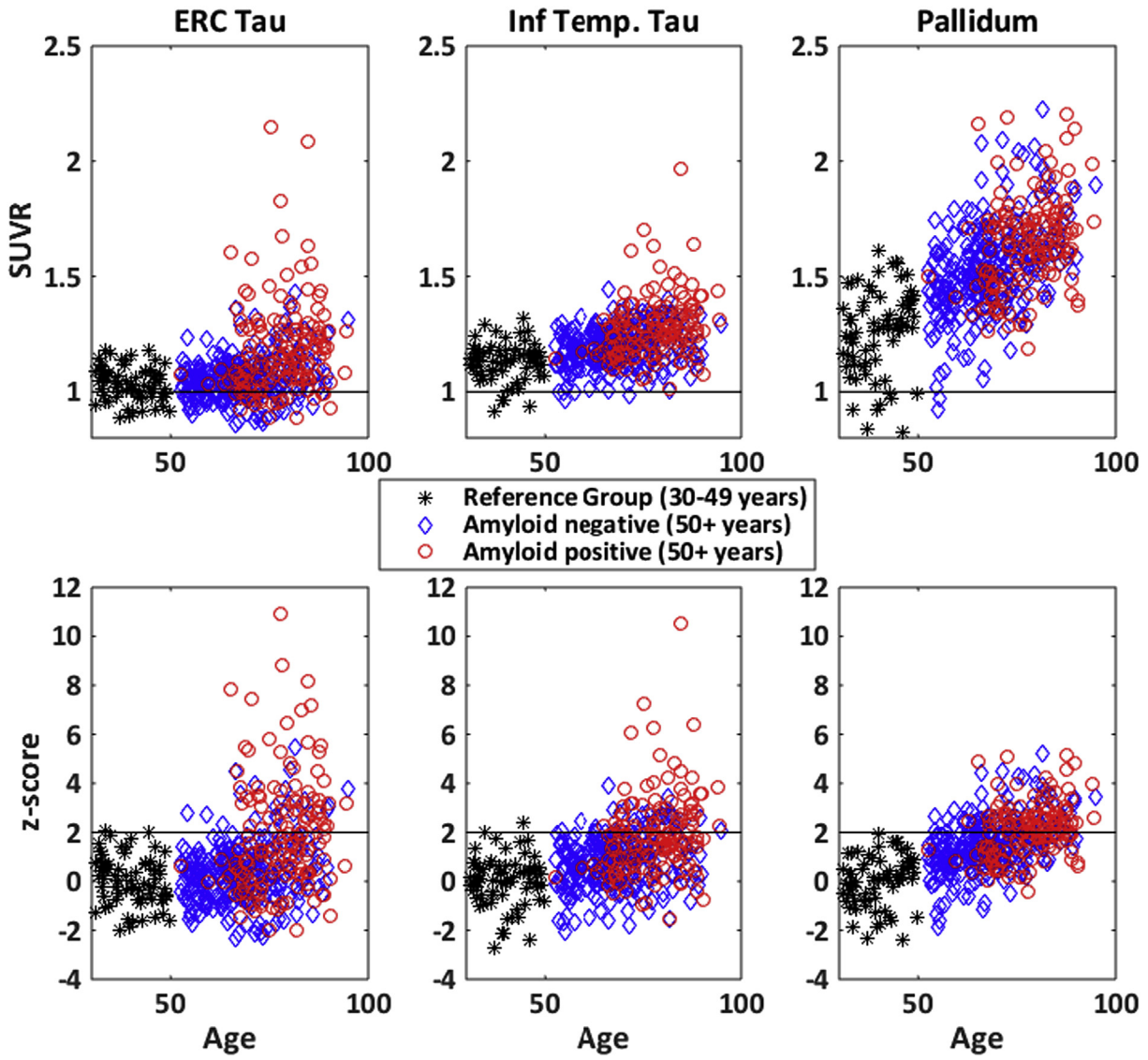

Fig. 3. Average tau-PET SUVR (top panels) and z-scores (bottom panels) in three regions. (Left panels) Entorhinal cortex tau; (middle panels) inferior temporal; (right panels) Pallidum. Color and symbols are used to indicate the reference group (30–49 years); amyloid positive (global amyloid $\geq$1.4; 50+ years) and amyloid negative (global amyloid$<$1.4; 50+ years). In the top panels, a line is shown at 1 to indicate background levels of tau-PET uptake (relative to median uptake in the cerebellar crus). In the bottom panels, a line is shown at 2 to indicate the cut point we used to determine tau positivity in the paper. Abbreviations: ERC, entorhinal cortex; SUVR, standardized uptake value ratio.

panel in Fig. 3) centers the data appropriately to observe that the ERC-tau signal may be more tightly associated with amyloid, that is, amyloid-positive individuals are likely to be ERC-tau positive compared to being inferior temporal tau positive. The standardization has a substantial effect on the nonspecific uptake seen in the pallidum. The pallidum SUVR has a higher mean and greater SD in the reference group (top panel), but after standardization, we can observe that there is a small age-related increase in the pallidum z-scores irrespective of the amyloid status (bottom panel).

To emphasize the change in the standardization and dynamic range of the regional values after the standardization of SUVR to z-scores, we computed average tau-PET SUVR and z-scores of the subregions into five composite larger regions in Fig. 4 as subgrouped in the panels of Figs. 1 and 2 (e.g., medial temporal signal is an average of the amygdala, ERC, hippocampus, and parahippocampal regions). Comparing raw SUVRs in the reference group, we observed lower SUVRs in the medial temporal lobes and the highest SUVRs in the occipital lobe. Comparing z-scores in the reference group, all regions have the same average values, that is, zero as expected. In the 50+ cohort, the relative ordering of the regions changed significantly after the standardization. Based on the pathology literature, medial temporal regions have greater

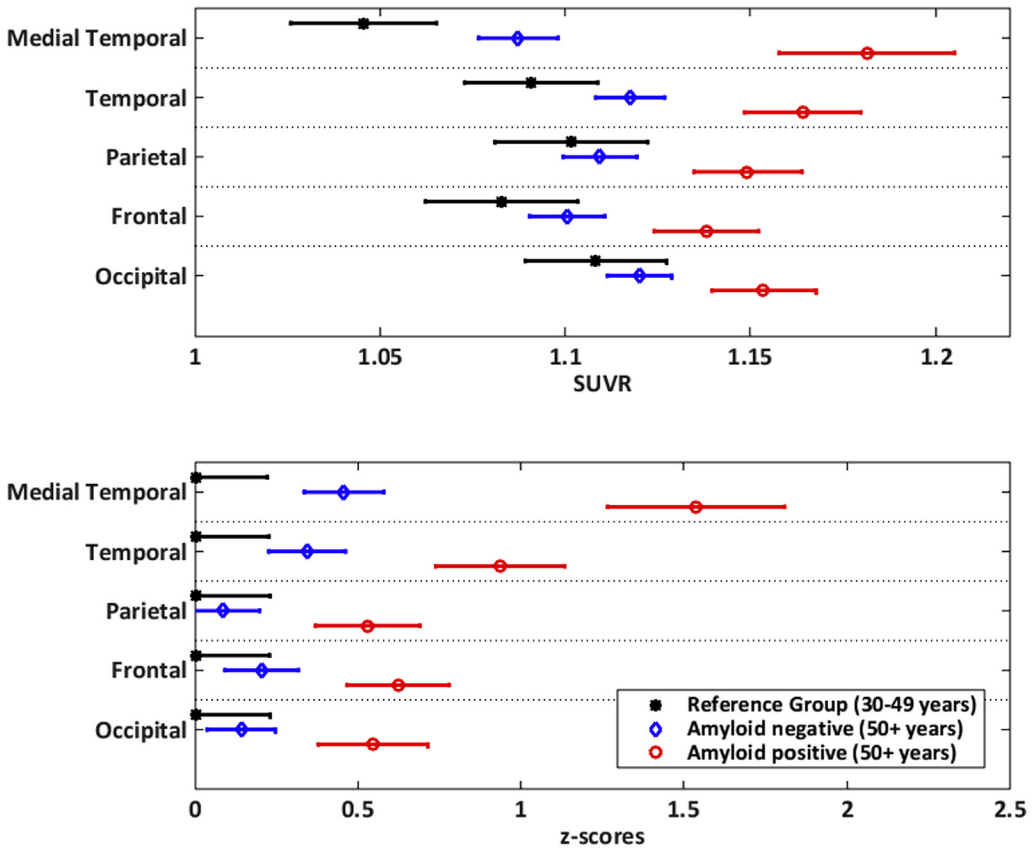

Fig. 4. Average tau-PET SUVR (top panel) and z-scores (bottom panel) in five composite regions. The means and 95% confidence intervals are shown as error bars for each region. The red circle indicates the amyloid positive 50+ (global amyloid $\geq$1.4), the blue diamond indicates the amyloid negative 50+ (global amyloid<1.4), and the black star indicates the reference group. The composite regions were created from the following subgroupings: medial temporal lobe is an average composite of amygdala, ERC, hippocampus, and parahippocampal gyrus. Temporal lobe is an average composite of fusiform, Heschl, insula, inferior, middle, and superior temporal, middle, and inferior temporal poles. Parietal is an average composite of angular, inferior and superior parietal, precuneus, and supramarginal. Frontal is an average composite of inferior (operculum, orbital, triangular), medial orbital, middle and middle orbital, superior, medial superior, superior orbital frontal gyri along with olfactory, rectus, and SMA. Occipital is an average composite of calcarine, cuneus, lingual, inferior, middle, and superior occipital lobes. Abbreviations: ERC, entorhinal cortex; SUVR, standardized uptake value ratio; SMA, supplementary motor area.

vulnerability to tau deposition than the rest of the brain with age and AD pathology. Comparing raw SUVR values across regions in the 50+ group, it may appear that occipital lobe has higher SUVR values in amyloid-negative individuals compared to medial temporal lobes. However, after standardization, the medial temporal z-scores are higher in both amyloid-positive and amyloid-negative individuals than occipital lobe z-scores as expected unlike the raw SUVR values.

3.2. Amyloid associations with regional tau-PET uptake

Correlations between tau-PET and global amyloid after adjusting for age are shown in Fig. 5. The magnitude of the association varied but was generally significant across regions. The highest correlations were in the medial temporal regions, specifically ERC. These associations were similar for partial volume–corrected data. In the 50+ individuals, we also categorized temporal regions as normal and abnormal based on z-score of 2 in Supplementary Fig. 1. We found that ERC-tau was more likely to be abnormal when an individual was amyloid positive (40%) compared to the inferior temporal tau (36%).

4. Discussion

We observed significant variability in the average regional tau-PET signal in the younger reference group. We used the reference group to standardize regional tau measurements in the 50+ cohort. Standardization of the data "realigns" the data such that the regional tau z-scores are informative of the disease process, that is, regions with high z-scores now coincide with regions correlated with amyloid deposition. There was significant association of global amyloid with regional tau-PET uptake throughout the brain after accounting for age with the greatest correlations in the medial temporal regions. Z-scores may not be necessary if mean tau SUVR values within a single region such as ERC are compared between groups of subjects such as in a randomized controlled trial.

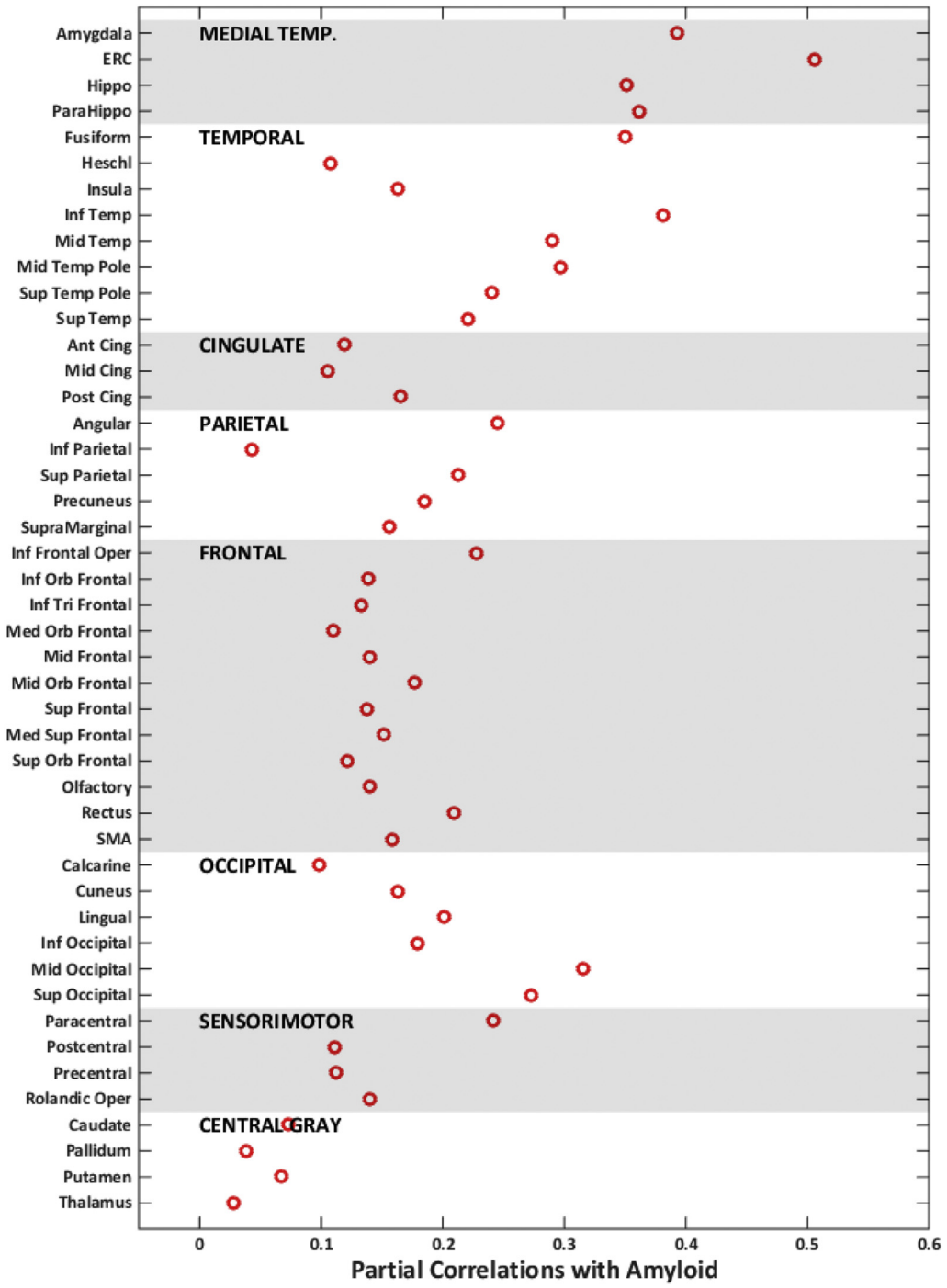

Fig. 5. Partial correlations with regional tau-PET in all 50+ individuals. Correlations with amyloid after adjusting for age are shown by red circles. Abbreviation: ERC, entorhinal cortex; SMA, supplementary motor area.

As tau-PET is increasingly used in research settings, average regional SUVRs will be used for differential diagnosis and understanding the pathological underpinnings of the cognitive impairment. Although group comparisons and correlation analyses within a given ROI are protected against the regional variation in average SUVR observed here, within-subject comparisons across different regional SUVRs may be misleading. This will also have a significant impact on determination of cut points for tau positivity as well as computation of composite-ROI tau-PET signatures as biomarkers [11]. With amyloid deposition, inter-ROI variation of mean SUVR has been less of a problem because there is significant amyloid deposition throughout the cortex early in the disease process, and averaging larger composite regions provides a reasonable estimate of the global amyloid load. On the other hand,

tau deposition appears to vary widely throughout the brain, and the effects of tau on cognition seem to be highly location specific [7].

Accounting for the regional variability of the average SUVR through standardization will greatly simplify data interpretation. This is illustrated by Fig. 4 where occipital SUVRs are highest compared to the other regions (~1.1). After z-score standardization, the tau z-scores are comparable to parietal and frontal lobes as mirroring what is seen in pathology studies. It may be debated whether the size of the region of interest will play an important role in the SUVR determination. In Supplementary Fig. 2, we illustrate the association between CV and mean SUVR versus average size of the region of interest in the reference group. Clearly, region size is not an important confounding factor.

Amyloid associations with tau-PET have recently been investigated [4–10]. In this study, we looked at the independent effects of amyloid on regional tau after accounting for age as also done by Scholl et al. [8]. The larger numbers and wider age ranges are strengths of the analyses presented here. There was significant association of amyloid with tau-PET uptake throughout the brain after accounting for age. Given our cohort of cognitively normal individuals most of whom likely have Braak neurofibrillary tangles (NFT) stages of IV or lower [26], the associations we found here between global amyloid and tau-PET throughout the brain (even regions affected in Braak V and Braak VI [27]) may suggest that there is simultaneous emergence of tau throughout the brain with increasing amyloid deposition. This idea concurs with the emerging data from our group [25] and others [5].

We found the strongest correlations in the medial temporal lobe suggesting that these regions may have heightened vulnerability to tau deposition associated with amyloid [28]. The use of inferior temporal lobe versus ERC-tau-PET as an AD tau-PET signature has been debated. Inferior temporal lobe has mean SUVR of 1.13 versus ERC has a mean SUVR of 1.03 in our reference group, which shows the effect of regional variability in the mean levels of tau SUVR. Standardization of the data by z-scoring aids in removing the nonuniform dynamic range throughout the brain and allows us to detect higher SUVR values in medial temporal lobes (Figs. 3 and 4). In addition, ERC-tau was slightly more likely to be abnormal when an individual was amyloid positive (40%) compared to the inferior temporal tau (36%). Due to greater sensitivity of ERC to amyloid, it may be suitable as AD-specific tau-PET signature. The correlation of ERC-tau uptake with the tau uptake in the rest of the brain is shown in Supplementary Fig. 3. ERC-tau is highly correlated with tau in other medial temporal regions and moderately correlated with tau levels in other regions in these cognitively normal individuals.

4.1. Strengths, limitations, and future studies

A major strength of this study is the availability of a reference group with PET scans sampled in a similar fashion as the cohort of interest. When a reference group is not available, statistical methods that allow for comparisons across the regions need to be considered, for example, correlations and group comparisons can be compared across all the brain regions but comparison of raw SUVR values between regions may be less meaningful. In a clinical trial setting, z-score may not be necessary if mean tau SUVR values within a single reporter region such as ERC are compared between treated and untreated subjects.

There are some limitations to this study. We designed the study with a limited scope. We combined left and right regions and did not look at the dose differences or quantification differences due to change in PET image processing. Also, we focused only on investigating the impact of amyloid on tau deposition. Future studies will be designed to investigate additional sources that may increase tau deposition other than amyloid.

Acknowledgments

The authors thank all the study participants and staff in the Mayo Clinic Study of Aging, Mayo Alzheimer's Disease Research Center, and Aging Dementia Imaging Research laboratory at the Mayo Clinic for making this study possible. The authors would like to also thank Stephen Weigand and Heather Wiste for their help with the preparation of the article. The authors would like to thank AVID Radiopharmaceuticals for the provision of AV-1451 precursor, chemistry production advice and oversight, and FDA regulatory cross-filing permission and documentation needed for this work.

This work was supported by NIH grants R01 NS097495 (PI: Vemuri), R00 AG37573 (PI: Vemuri), U01 AG06786 (PI: Petersen), P50 AG16574/P1 (PI: Vemuri), P50 AG16574 (PI: Petersen), R01 AG034676 (PI: Rocca), R01 AG11378 (PI: Jack), R01 AG041851 (PIs: Jack and Knopman); the Gerald and Henrietta Rauenhorst Foundation grant, the Alexander Family Alzheimer's Disease Research Professorship of the Mayo Foundation, the Elsie and Marvin Dekelboum Family Foundation, USA, and Opus Building NIH grant C06 RR018898. The funding sources were not involved in the article review or approval.

The authors report no conflicts of interest.

Supplementary data

Supplementary data related to this article can be found at http://dx.doi.org/10.1016/j.dadm.2016.12.010.

RESEARCH IN CONTEXT

1. Systematic review: Tau-PET ligands have recently been developed, with AV1451 being the most studied at this point. The effect of amyloid on tau and the neuroanatomical variability of tau-PET uptake across subject and patient groups are currently being thoroughly investigated.
2. Interpretation: The average SUVR values are variable in different brain areas. Standardization of regional tau-PET SUVR (here with z-scores) is therefore recommended. Amyloid and tau-PET uptake were associated throughout the brain, with the highest correlations found in medial temporal regions. Although it is not a high SUVR region, the high age-independent correlation with amyloid and high z-scores in amyloid-positive individuals after standardization show that ERC-tau may be useful as an AD-specific tau-PET signature.
3. Future directions: More extensive work will be undertaken to study the effect of PET acquisition, processing, and quantification on SUVR. Methods for measuring tau-PET biomarkers will be developed that account for the variability in the data.

References

[1] Klunk WE, Engler H, Nordberg A, Wang Y, Blomqvist G, Holt DP, et al. Imaging brain amyloid in Alzheimer's disease with Pittsburgh Compound-B. Ann Neurol 2004;55:306–19.

[2] Ikonomovic MD, Klunk WE, Abrahamson EE, Mathis CA, Price JC, Tsopelas ND, et al. Post-mortem correlates of in vivo PiB-PET amyloid imaging in a typical case of Alzheimer's disease. Brain 2008; 131:1630–45.

[3] Bacskai BJ, Frosch MP, Freeman SH, Raymond SB, Augustinack JC, Johnson KA, et al. Molecular imaging with Pittsburgh Compound B confirmed at autopsy: a case report. Arch Neurol 2007;64:431–4.

[4] Chien DT, Bahri S, Szardenings AK, Walsh JC, Mu F, Su MY, et al. Early clinical PET imaging results with the novel PHF-tau radioligand [F-18]-T807. J Alzheimers Dis 2013;34:457–68.

[5] Brier MR, Gordon B, Friedrichsen K, McCarthy J, Stern A, Christensen J, et al. Tau and Aβ imaging, CSF measures, and cognition in Alzheimer's disease. Sci Transl Med 2016;8:338ra66.

[6] Johnson KA, Schultz A, Betensky RA, Becker JA, Sepulcre J, Rentz D, et al. Tau positron emission tomographic imaging in aging and early Alzheimer disease. Ann Neurol 2016;79:110–9.

[7] Ossenkoppele R, Schonhaut DR, Scholl M, Lockhart SN, Ayakta N, Baker SL, et al. Tau PET patterns mirror clinical and neuroanatomical variability in Alzheimer's disease. Brain 2016;139:1551–67.

[8] Scholl M, Lockhart SN, Schonhaut DR, O'Neil JP, Janabi M, Ossenkoppele R, et al. PET imaging of tau deposition in the aging human brain. Neuron 2016;89:971–82.

[9] Schwarz AJ, Yu P, Miller BB, Shcherbinin S, Dickson J, Navitsky M, et al. Regional profiles of the candidate tau PET ligand 18F-AV-1451 recapitulate key features of Braak histopathological stages. Brain 2016;139:1539–50.

[10] Cho H, Choi JY, Hwang MS, Lee JH, Kim YJ, Lee HM, et al. Tau PET in Alzheimer disease and mild cognitive impairment. Neurology 2016; 87:375–83.

[11] Jack CR Jr, Bennett DA, Blennow K, Carrillo MC, Feldman HH, Frisoni GB, et al. A/T/N: An unbiased descriptive classification scheme for Alzheimer disease biomarkers. Neurology 2016; 87:539–47.

[12] Lowe VJ, Curran G, Fang P, Liesinger AM, Josephs KA, Parisi JE, et al. An autoradiographic evaluation of AV-1451 Tau PET in dementia. Acta Neuropathol Commun 2016;4:58.

[13] Marquie M, Normandin MD, Vanderburg CR, Costantino IM, Bien EA, Rycyna LG, et al. Validating novel tau positron emission tomography tracer [F-18]-AV-1451 (T807) on postmortem brain tissue. Ann Neurol 2015;78:787–800.

[14] Xia CF, Arteaga J, Chen G, Gangadharmath U, Gomez LF, Kasi D, et al. [(18)F]T807, a novel tau positron emission tomography imaging agent for Alzheimer's disease. Alzheimers Dement 2013;9:666–76.

[15] Tong S, Alessio AM, Kinahan PE. Image reconstruction for PET/CT scanners: past achievements and future challenges. Imaging Med 2010;2:529–45.

[16] Su Y, Blazey TM, Snyder AZ, Raichle ME, Marcus DS, Ances BM, et al. Partial volume correction in quantitative amyloid imaging. Neuroimage 2015;107:55–64.

[17] Schmidt ME, Chiao P, Klein G, Matthews D, Thurfjell L, Cole PE, et al. The influence of biological and technical factors on quantitative analysis of amyloid PET: points to consider and recommendations for controlling variability in longitudinal data. Alzheimers Dement 2015; 11:1050–68.

[18] Rocca WA, Yawn BP, St. Sauver JL, Grossardt BR, Melton LJ. History of the Rochester Epidemiology Project: half a century of medical records linkage in a US population. Mayo Clin Proc 2012;87:1202–13.

[19] St Sauver JL, Grossardt BR, Leibson CL, Yawn BP, Melton LJ 3rd, Rocca WA. Generalizability of epidemiological findings and public health decisions: an illustration from the Rochester Epidemiology Project. Mayo Clin Proc 2012;87:151–60.

[20] Petersen RC, Roberts RO, Knopman DS, Geda YE, Cha RH, Pankratz VS, et al. Prevalence of mild cognitive impairment is higher in men. The Mayo Clinic Study of Aging. Neurology 2010; 75:889–97.

[21] Roberts RO, Geda YE, Knopman DS, Cha RH, Pankratz VS, Boeve BF, et al. The incidence of MCI differs by subtype and is higher in men: The Mayo Clinic Study of Aging. Neurology 2012;78:342–51.

[22] Jack CR Jr, Lowe VJ, Senjem ML, Weigand SD, Kemp BJ, Shiung MM, et al. 11C PiB and structural MRI provide complementary information in imaging of Alzheimer's disease and amnestic mild cognitive impairment. Brain 2008;131:665–80.

[23] Lopresti BJ, Klunk WE, Mathis CA, Hoge JA, Ziolko SK, Lu X, et al. Simplified quantification of Pittsburgh Compound B amyloid imaging PET studies: a comparative analysis. J Nucl Med 2005;46:1959–72.

[24] Jack CR, Wiste HJ, Weigand S, Knopman D, Mielke MM, Vemuri P, et al. Different definitions of neurodegeneration produce similar frequencies of amyloid and neurodegeneration biomarker groups by age among cognitively non-impaired individuals. Brain 2015; 138:3747–59.

[25] Lowe V, Wiste HJ, Pandey M, Senjem M, Boeve B, Josephs KA, et al. Tau-PET imaging with AV-1451 in Alzheimer's disease. in Human Amyloid Imaging. 2016. Miami Beach, FL.

[26] Braak H, Braak E. Frequency of stages of Alzheimer-related lesions in different age categories. Neurobiol Aging 1997; 18:351–7.

[27] Braak H, Braak E. Neuropathological stageing of Alzheimer-related changes. Acta Neuropathol 1991;82:239–59.

[28] Stranahan AM, Mattson MP. Selective vulnerability of neurons in layer II of the entorhinal cortex during aging and Alzheimer's disease. Neural Plast 2010;2010:108190.